CORRELATION OF FLOODING VELOCITIES IN PLATE COLUMNS WITHOUT DOWNCOMER

Yasuharu AKAGI

Department of Applied Chemistry, Okayama College of Science, Okayama

Abstract

Flooding velocities of plate columns are an upper limit of stable operational range, and also a very important factor for design and operation of the plate columns. In order to study the flooding velocities, various types of plate columns without downcomer (sieve trays, sieve trays with holes of two different diameters, turbo-grid trays, two types of ripple trays and rotational-current trays) were used.

The flooding velocities of these trays were found to be well correlated by modifing the correlation of flooding velocities in the packed columns which was proposed by Zenz and Eckert. The shape factor in the correlation has its own correlation according to each type of the trays mentioned above.

Introduction

Flooding velocities of plate columns are an upper limit of stable operational range, and also a very important factor for design and operation of the plate columns. It is generally considered that the flooding of plate columns without downcomer occurs when the pressure drop or the entrainment increases rapidly.

Flooding velocities of the plate columns without downcomer have been mainly studied on turbo-grid trays and sieve trays[2,3,6,9]. Experimental data of other types of trays have been rarely published.

The present paper is concerned with flooding velocities of trays of the countercurrent type without downcomer, such as sieve trays, sieve trays with holes of two different diameters, turbo-grid trays, two types of ripple trays and rotational-current trays. Flooding velocities of these trays are determined experimentally by the pressure drop curves plotted for gas velocities. The flooding velocities of these trays were found to be well correlated by modifing the correlation of flooding velocities in the packed columns which was proposed by Zenz and Eckert[11].

1. Flooding Velocities of Packed Columns in Previous Works

Sherwood et al.[7] reported that flooding velocities in packed columns can be graphically correlated, if the following coordinate is used.

$$\frac{U_{GC}^2}{g}\frac{\rho_G}{\rho_L}\mu_L^{0.2}\frac{a}{\varepsilon^3}\ \text{(ordinate) vs.}\ \left(\frac{L_{MF}}{G_{MF}}\right)\left(\frac{\rho_G}{\rho_L}\right)^{0.5}\text{(abscissa)} \qquad (1)$$

Lobo et al.[4] studied on the packing factor, a/ε^3. And they graphically correlated the flooding velocities using Sherwood's coordinate and the new packing factors. Zenz[10] also studied flooding velocities in packed columns based on his experimental results.

In the graphical correlation using Sherwood's coordinate, the flooding velocities must be calculated by the trial and error method. This calculation is practically inconvenient.

Zenz and Eckert[11] made transformation of Sherwood's coordinate into the following form.

$$\text{(abscissa) (ordinate)}^{0.5} \text{ vs. } \text{(ordinate)}^{0.5} \qquad (2)$$

that is

$$\left.\begin{aligned} X &= U_{LF}\left(\frac{\mu_L^{0.2}}{g}\frac{a}{\varepsilon^3}\right)^{0.5} \\ Y &= U_{GF}\left(\frac{\rho_G}{\rho_L}\frac{\mu_L^{0.2}}{g}\frac{a}{\varepsilon^3}\right)^{0.5} \end{aligned}\right\} \qquad (3)$$

Thus gas velocities are not included in abscissa.

Using the new coordinate, the results of the flooding velocities in the previous works are presented by **Fig. 1**. Packing factors reported by Lobo et al. were used in this rearrangement.

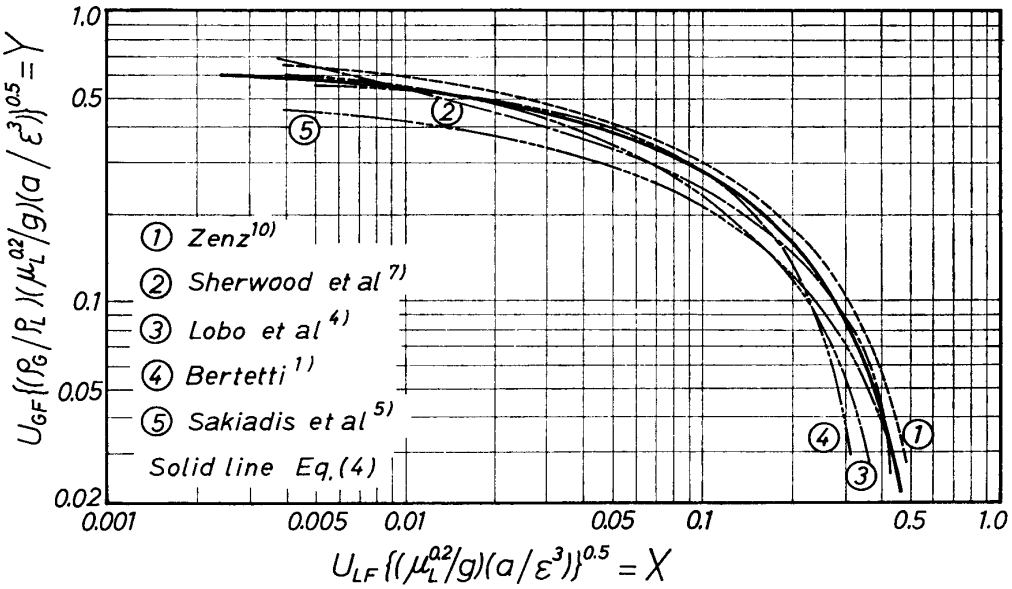

Fig. 1 Correlation of flooding velocities in packed columns

The curves 4 and 5 show the results of air-water system. The results calculated in other systems are similar to the curves 4 and 5 because the effects of physical properties are similar to Eq. (3).

2. Experimental Apparatus and Procedures

2.1 Trays

In the present work, seven types of trays (Type-A, B, C, D, E, F and G) were used. The dimensions of these trays are shown in **Table 1** and **Fig. 2**. In all the types of trays, some dozen trays were used.

A sieve tray (type A) have the holes arranged in triangular form. A sieve tray with holes of two different diameters (type B) is constructed with two kinds of holes which is

Table 1 Ranges of tray dimensions and physical properties

Type of tray		d_e [m]	A_h/A_c [—]	ρ_L [kg/m³]	ρ_G [kg/m³]	μ_L [kg/m hr] (c. p.)	μ_G [kg/m hr] (c. p.)	σ [kg/hr²] (dyn/cm)
Sieve tray (A)		0.0038 ~0.02	0.119 ~0.370	844 ~1165	1.2	2.9~52 (0.8~14.5)	0.065 (0.018)	4.8~9.6×10⁵ (37~74)
Sieve tray with holes of two different diameters (B)		0.003 ~0.02	0.095 ~0.325	818 ~1188	1.2	2.9~75.6 (0.8~21)	0.065 (0.018)	3.5~9.6×10⁵ (27~74)
Turbo-grid tray (C)		0.004 ~0.024	0.164 ~0.360	837 ~1170	1.2	3.6~56 (1~15.6)	0.065 (0.018)	5.3~9.6×10⁵ (41~74)
Ripple tray	Rectangular type (D)	0.0035 ~0.012	0.103 ~0.367	876 ~1164	1.2	3.6~50 (1~14)	0.065 (0.018)	5.3~9.6×10⁵ (41~74)
	Triangular type (E)	0.0035 ~0.012	0.095 ~0.335	897 ~1163	1.2	3.6~72.4 (1~20)	0.065 (0.018)	5.9~9.6×10⁵ (45~74)
Rotational-current tray	U. G. T. (F) D. G. T. (G)	0.0054 ~0.011	0.103 ~0.286	840 ~1170	1.2	2.9~54 (0.8~15)	0.065 (0.018)	4.5~9.6×10⁵ (35~74)

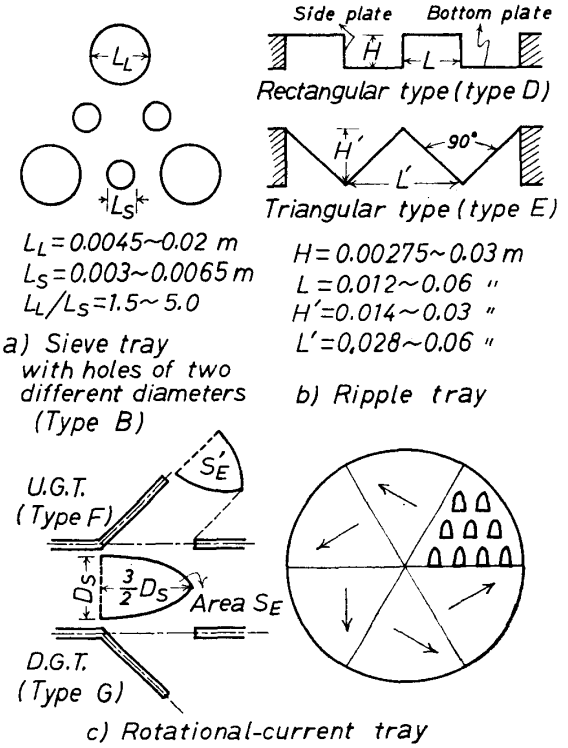

Fig. 2 Structure of trays used

arranged in triangular form as shown in Fig. 2(a). The hole diameter, d_e of this tray is the hydraulic diameter calculated from all the holes of a tray. In a turbo-grid tray (type C), the hole diameter, d_e is twice the slot width.

As regards the ripple trays, the trays of simple structure were used and thus the effects

of geometrical factors will be well understood. Two types of trays, that is, one is a rectangular type (type D) and the other a triangular type (type E) as shown in Fig. 2 (b), were experimented. The side plates in type D were not perforated. A_h/A_c was calculated by the area projected on a plane.

A rotational-current tray[8] is shown in Fig. 2(c). The shape of holes in the tray represents a half of ellipse and each hole has a guide of the same type of angle 45°. The froth on the tray rotates due to the arrangement of holes as shown in the figure. This tray was experimented in both of the two cases of the upper guide (U. G. T.) and the down guide (D. G. T.).
In Table 1, d_e and A_h/A_c were obtained by the area S'_E.

2. 2 Apparatus and Procedures

The schematic flowsheet of the experimental apparatus is shown in **Fig. 3(a)**. Liquids are

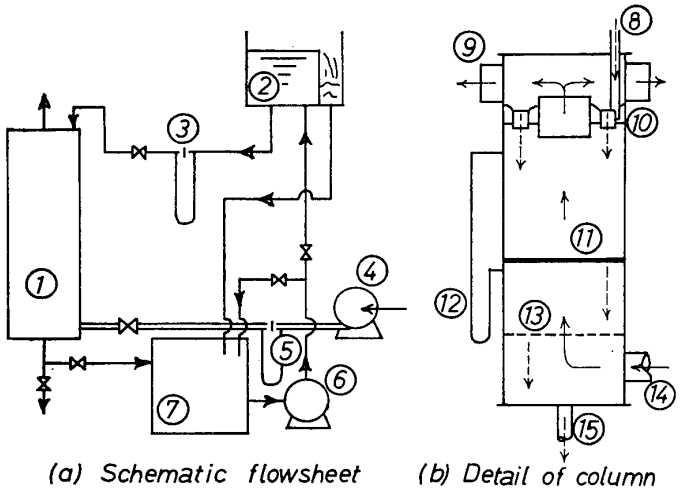

1. tower 2. head tank 3. liquid flow meter 4. blower 5. gas flow meter 6. pump 7. feed tank 8. liquid inlet 9. gas outlet 10. liquid distributor 11. tray 12. manometer 13. gas distributor 14. gas inlet 15. liquid outlet

Fig. 3 Experimental apparatus

stored in a feed tank ⑦ and pumped up into a constant head tank ② by a circulation pump ⑥, from which these are fed to a column ① at a liquid inlet ⑧ through a flow meter ③. The liquids flowing down from a liquid distributor ⑩ return to the feed tank through a liquid outlet ⑮ after getting in contact with the air on the tray ⑪.

On the other hand, air from a blower ④ is pumped into the column through a flow meter ⑤ and a gas inlet ⑭ and then distributed by a gas distributor ⑬ and goes out of a gas outlet ⑨ after getting in contact with the liquid on the tray.

The detail of the column ① is shown in **Fig. 3(b)**. The column which houses a test tray of 0.15 m diameter is made of transparent vinyl chloride resin. Visual observation is possible.

At each run, gas velocities were widely varied at several constant liquid velocities. Pressure drop of gas through a tray was measured by the precision manometer ⑫. Gas and liquid velocities varied from 500 to 20000 $m^3/m^2\ hr$ and from 1.7 to 30 $m^3/m^2\ hr$, respectively.

The experiments were performed water-air, aqueous glycerin solution-air and aqueous methanol solution-air systems. The ranges of the variables are shown in Table 1.

3. Experimental Results

3. 1 Determination of flooding point

Fig. 4 shows the relations between pressure drop and gas velocities based on an empty

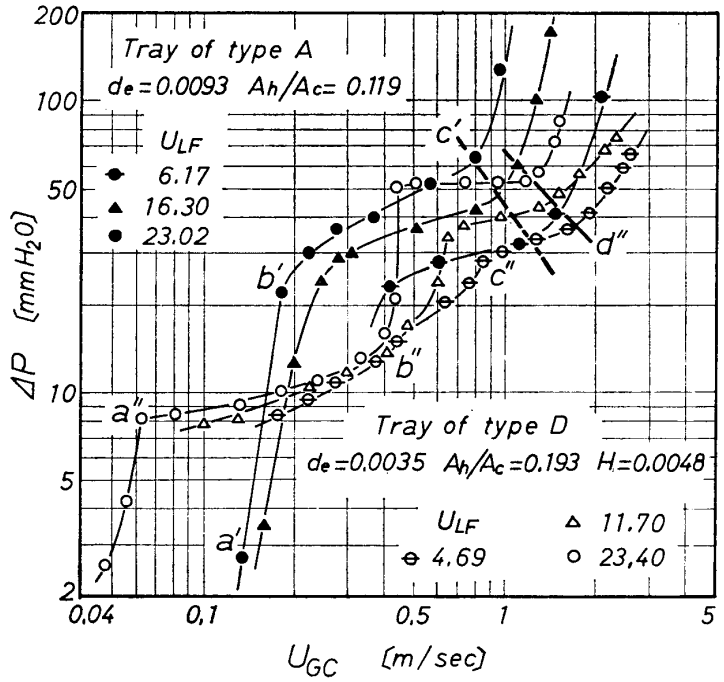

Fig. 4 Typical pressure drop curves in air-water system

column both for type A and type D. At the gas velocity below point a' in type A, the falling liquids do not stagnate on the tray. For region a'-b', pressure drop increases rapidly. The liquids stagnate at this region and the foaming layer is observed on the tray. Both the froth height and the pressure drop increase slowly in region b'-c'. The froth height increases rapidly and at the same time the entrainment increases at the gas velocity above point c'. Region b'-c', as mentioned above, is the stable operational range and the flooding points are determined from point c'. In the types B, C, F and G, the flooding points are determined in the same way.

In the type D, the liquids begin to stagnate on the bottom plates as can be seen from Fig. 2(b) at point a''. The liquid holdups on the bottom plates increase slowly at region a''-b'' and the liquids stagnate on whole area of the tray in region b''-c''. Region c''-d'' is the stable operational range. The flooding points in this tray are determined from point d''. In the type E, the flooding points are determined in the same way.

3.2 Effects of tray dimensions and physical properties on flooding velocity

Fig. 5 shows an example of the effects of d_e and A_h/A_c on flooding gas velocities. It is seen that the effect of d_e does not appear in the range investigated and the flooding gas velocities increase linearly with the increase of A_h/A_c. This trends are common to all types of trays. Furthermore, H affects to the flooding velocities in addition to A_h/A_c in the type D. In this case the flooding gas velocities increase with the increase of H. Because the flowing down of the liquid through the tray of large H is smooth, this tray will be stably operated up to large gas velocities.

Fig. 5 also shows the effect of μ_L for the flooding gas velocities. It is seen that μ_L has little effect for the flooding velocities. Surface tension of the liquid is found to have also little effect for the flooding velocities. The flooded foaming layer is unstable, and oscillates. Furthermore, the situation in which the fall of liquid and the rise of gas occur alternately is

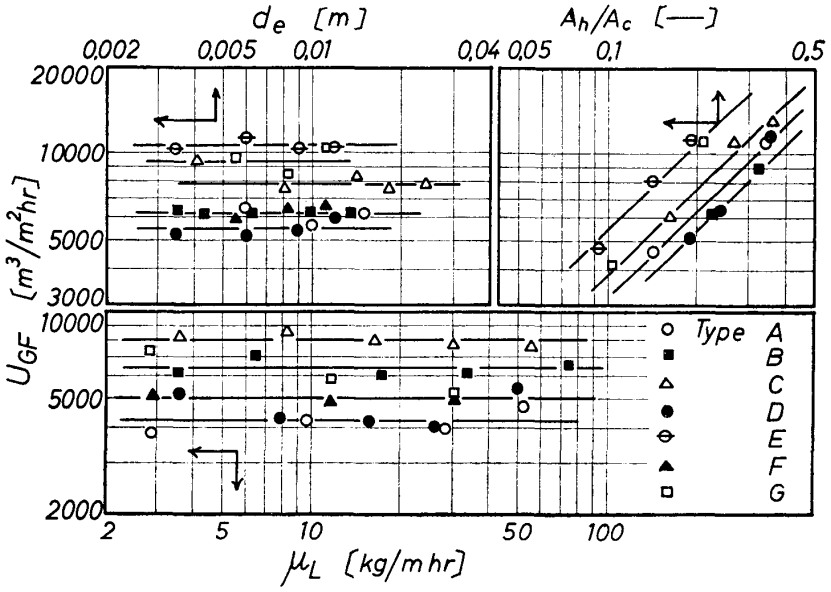

Fig. 5 Effects of d_e, A_h/A_c and μ_L for flooding velocities

seen in many trays. Therefore, the effect of these physical properties will be not appeared.

4. Correlation of Flooding Velocities

It can be considered that the several curves in Fig. 1 are represented by the solid line in the figure. This curved line is presented by the following equation.

$$Y = exp(2.9/ln\ X) \tag{4}$$

As the plate columns without downcomer are the contactor of the column type in which gas and liquid flow countercurrently in the same way as in the packed columns, it may be considered that the flooding phenomena of both contactors are similar. Therefore, the flooding velocities of the columns will be correlated by Eq. (4).

4.1 Correlations

As discussed in **3.2**, the flooding gas velocities are not affected by d_e, μ_L and σ, but are affected by A_h/A_c. In the type D, H affects in addition to A_h/A_c. Considering the relations of Eq. (3) and the experimental results, X and Y of Eq. (4) may be presented by using the following correlation for these trays.

$$\left.\begin{aligned} X &= U_{LF}\left(\frac{1}{g} S_F\right)^{0.5} \\ Y &= U_{GF}\left(\frac{\rho_G}{\rho_L} \frac{1}{g} S_F\right)^{0.5} \end{aligned}\right\} \tag{5}$$

Where S_F represents the so-called shape factor corresponding to a/ε^3 in Eq. (3) and it will be expected that S_F is correlated by A_h/A_c and H.

Hence, the procedures for search of S_F can be shown as follows. The flooding velocities and the physical properties of gas and liquid are substituted in Eq. (5). Furthermore, a values

of S_F is assumed and substituted in Eq. (5), and then Eq. (4) is calculated by using the values of X and Y of Eq. (5). By the repetition of this procedure, the value of S_F that satisfies Eq. (4) is determined by a computer. The correlations of S_F of various trays are shown in **Fig. 6** and **Table 2**.

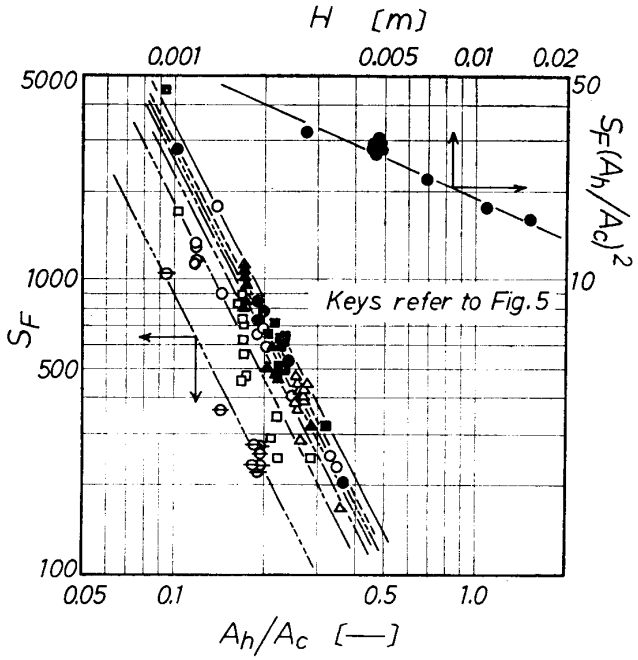

Fig. 6 Correlations of shape factors

Table 2 Correlation of S_F

Tray type		S_F
A		$\frac{23}{(A_h/A_c)^2}$
B		$\frac{33}{(A_h/A_c)^2}$
C		$\frac{26}{(A_h/A_c)^2}$
D		$\frac{1.9}{(A_h/A_c)^2 H^{0.5}}\left(\frac{15.5\sim36}{(A_h/A_c)^2}\right)^*$
E		$\frac{9.1}{(A_h/A_c)^2}$
F		$\frac{27}{(A_h/A_c)^2}$
G		$\frac{18}{(A_h/A_c)^2}$
A	Uchiyama et al.[9]	$\frac{4\sim20}{(A_h/A_c)^2}$
	Eduljee[2]	$\frac{3\sim100}{(A_h/A_c)^2}$
C	Kasatkin et al.[3]	$\frac{14\sim28}{(A_h/A_c)^2}$
	Uchiyama et al.[9]	$\frac{9\sim16}{(A_h/A_c)^2}$
	Eduljee[2]	$\frac{0.14\sim40}{(A_h/A_c)^2}$

* $H=0.00275\sim0.03\,m$

As shown in Eqs. (4) and (5), the flooding velocities become the large values when S_F values become small. The measured values of the flooding velocities are presented in **Fig. 7** by

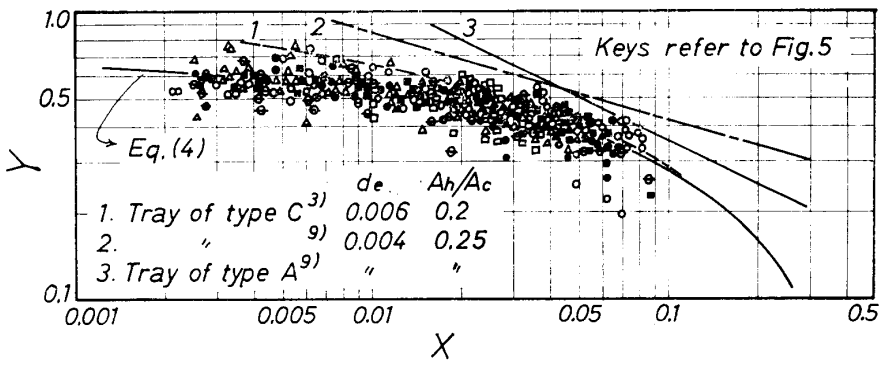

Fig. 7 Comparisons of measured, calculated values and the results of previous works in flooding velocities

using Eqs. (4) and (5) and S_F values in Table 2, and agree well with Eq. (4).

4.2 Comparison with the previous works and proposed values of S_F

Sanga[6] reported that the flooding in sieve trays without downcomer occurs when the foaming layer on the tray becomes unstable as a result of causing swinging or rotating motion, and that the flooding velocities can be correlated by the wet pressure drop.

Kasatkin et al[3]. reported a correlation for turbo-grid trays. And Eduljee[2] and Uchiyama et al[9]. reported the correlations for sieve and turbo-grid trays respectively.

By using these experimental results, the values of S_F calculated by Eqs. (4) and (5) are shown in Table 2. As the range of variables of each experiment does not agree, the rigid comparisons with each other are difficult. Therefore, the S_F values of these experiments for the range of variables the same as used in the present work have been compared with those of the present work. The results of Uchiyama et al. and Kasatkin et al. are shown in Fig. 7. Kasatkin's correlation is very similar to Eq. (4) except the effect of d_e.

Conclusions

1. Flooding velocities of plate columns without downcomer and packed columns are well correlated by Eq. (4). X and Y in Eq. (4) are different in both them, and given by Eq. (5) in plate columns without downcomer and given by Eq. (3) in packed columns.
2. The shape factors, S_F are functions of A_h/A_c only. S_F of the type D, however, are affected by H. S_F values of each type of trays are shown in Table 2.
3. Upper velocities of the stable operational range of plate columns without downcomer increase with the decrease of S_F and are not affected by d_e, μ_L and σ.

Acknowledgement

I wish to thank Professor T. Takahashi of Okayama University for many helpful suggestions during the course of this work.

Nomenclature

a = *surface area of packing* [m^2/m^3]
d_e = *equivalent diameter of hole* [m]
D_S = *short diameter of hole of rotational-current tray* [m]
D_T = *column diameter* [m]
A_h/A_c = *ratio of total hole or slot area to tray area* [——]
G_{MF} = *flooding gas mass velocity* [kg/m^2hr]
H, H' = *wave depth of ripple tray, refer to Fig. 2* [m]
L, L' = *wave pitch of ripple tray, refer to Fig. 2* [m]
L_{MF} = *flooding liquid mass velocity* [kg/m^2hr]
ΔP = *pressure drop through a tray* [mmH_2O]
S_E = *area of a hole of rotational-current tray, refer to Fig. 2* [m^2]
S'_E = *projected area of S_F, refer to Fig. 2* [m^2]
S_F = *shape factor in flooding* [——]

U_{GC} = *superficial gas velocity based on empty column section* 〔*m/sec*〕
U_{GF} = *flooding gas velocity* 〔m^3/m^2hr〕
U_{LF} = *flooding liquid velocity* 〔m^3/m^2hr〕
ε = *void fraction of packed column* 〔——〕
μ_G = *viscosity of gas* 〔*kg/m hr*〕
μ_L = *viscosity of liquid* 〔*kg/m hr*〕
ρ_G = *density of gas* 〔kg/m^3〕
ρ_L = *density of liquid* 〔kg/m^3〕
σ = *surface tension of liquid* 〔kg/hr^2〕

Literature cited

1) Bertetti, J. W., *Trans. A. I. Ch. E.*, 38, 1023 (1942)
2) Eduljee, H. E., *Brit. Chem. Eng.*, 11, 1519 (1966)
3) Kasatkin, A. G., Yu. I. Dytnerski and S. U. Umarov, *Khim. Prom.*, No. 3, 166 (1958)
4) Lobo, W. E., L. Friend, F. Hashmall and F. A. Zenz, *Trans. A. I. Ch. E.*, 41, 693 (1945)
5) Sakiadis, B, C. and A. I. Johnson, *Ind. Eng. Chem.*, 46, 1229 (1954)
6) Sanga, S., *Kagaku Kogaku*, 27, 162 (1963)
7) Sherwood, T. K., G. H. Shipley and F. A. L. Holloway, *Ind. Eng. Chem.*, 30, 765 (1938)
8) Takahashi, T. and Y. Akagi, *Kagaku Kogaku*, 31, 600 (1967)
9) Uchiyama, H., K. Hirao and N. Meno, *Kagaku kogaku*, 35, 116 (1971)
10) Zenz, F. A., *Chem. Eng. Progr.*, 43, 415 (1947)
11) Zenz, F. A. and R. A. Eckert, *Petrol. Refiner*, 40, 130 (1961)